

In-situ Mechanical Calibration for Vision-based Tactile Sensors

Can Zhao¹, Jieji Ren², Hexi Yu¹, and Daolin Ma^{1*}

Abstract—This paper proposes a novel approach to conduct routine calibration for the changing mechanical parameters over time of a vision-based tactile sensor, without disassembling its overall structure, i.e., *in-situ mechanical calibration*.

Calibration for mechanical parameters, Young’s modulus and Poisson’s ratio, of a tactile sensor’s sensing elastomer, is crucial for its force perception capabilities. However, there are few methods that can retrieve values of these parameters both accurately and conveniently. To address this problem, we propose an in-situ approach to calibrate mechanical parameters other than the verbose traditional evaluation process. This method incorporates the deformation sensing capability of the sensor, the accurate force sensing capability of a force/torque sensor, and most importantly, the deformation-force relationship for an indentation with embedded mechanical parameters of the elastomers. We also present the indentation test setup and the complete pipeline to extract Young’s modulus and Poisson’s ratio from experimental results.

We validate the method by comparing the indentation depths simulated through finite element analysis (FEA) using the calibrated parameters with the indentation depths measured in real experiments. Furthermore, superior contact force distribution can be achieved with the accurate mechanical parameters.

The proposed method provides the theoretical basis for accurate, lifelong routine calibration, whether weekly or even daily, which can enhance the applications of tactile sensors in real manipulation scenarios.

I. INTRODUCTION

In this work, we address the problem of routinely calibrating the mechanical parameters of a tactile sensor’s sensing elastomer without ripping it off from the sensor, which we refer to as *in-situ mechanical calibration*.

Vision-based tactile sensors have been receiving greater attention for their high spatial resolution and multi-modal sensing capabilities [1]–[3]. Typically, these sensors comprise of a sensing elastomer and an inbuilt camera, which estimate the contact deformation through observing the color change of the elastomer surface. Accurate force distribution can be reconstructed when mechanical parameters of the elastomer are known. Young’s modulus and Poisson’s ratio, which are independent of each other, are the two critical mechanical parameters of soft material. Here, (1) **Young’s modulus** (E) describes the stiffness of elastomers, and characterizes the relationship between the axial strain in the linear elastic domain and the tensile/compressive stress. (2)

*This work was supported by NSFC (Grant No. 12272220), the Oceanic Interdisciplinary Program of Shanghai Jiao Tong University (project number SL2021MS017) and CATL Shanghai Research Institute.

¹Daolin Ma, Can Zhao, and Hexi Yu are with the School of Naval Architecture, Ocean & Civil Engineering, Shanghai Jiao Tong University, Shanghai, China. E-mail: daolinma, can.zhxx, yhx19990916@sjtu.edu.cn

²Jieji Ren is with the School of Mechanical Engineering, Shanghai Jiao Tong University, Shanghai, China. E-mail: jieji.ren@sjtu.edu.cn

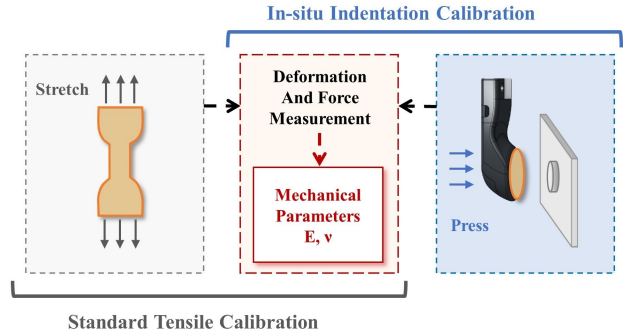


Fig. 1. In-situ Indentation calibration vs standard Tensile calibration.

Poisson’s ratio (ν) measures the Poisson effect, reflecting how much the flexible sensing elastomers deform in the plane perpendicular to the applied force.

Therefore, reliable mechanical parameters of sensing elastomers are critical for vision-based tactile sensors. Accurate contact force estimation and various force-based tactile perceptions can only be achieved when precise mechanical parameters are available [4], [5]. However, it has been verified that the mechanical behavior of elastomers is strongly affected by aging, typically leading to a stiffer and more brittle behavior [6]. For example, Placet and Delobelle’s study [7] suggests that the Young’s modulus for small strain behavior may increase by up to 50% with sample age, while R. Hopf et al. [8] demonstrate that the time span between sample preparation and testing affects the large strain nonlinear behavior, even within a four-week period. Therefore, regular mechanical calibration of tactile sensors using elastomers is crucial for practical applications.

Traditionally, there exists the standard procedure for calibrating soft materials, namely tensile test. This method relies on using an accurate force gauge to measure the tensile force, while digital image correlation technology (DIC) is used to measure the planar strain field. Using these measurements, E and ν can be calculated. However, this method can be cumbersome, as it requires the preparation of standalone dog-bone-shaped elastomer samples that are specially painted, making it impractical for calibrating elastomers that are already assembled on the sensor, as shown in Fig.1.

To address this issue, we present *In-situ calibration*, a novel approach to calibrate the mechanical parameters of soft sensing elastomers for vision-based tactile sensors both accurately and conveniently with a series of indentation tests. This approach leverages the sensor’s built-in deformation measurement capability with the accurate force measurement capability of an off-the-shelf force sensor, and core to this

method is to untangle (E) and (ν) since the two are intricately embedded in the force and deformation measurements for indentations.

The proposed approach can be employed for life-long calibration and doesn't necessitate tearing apart the sensor's overall structure. The on-demand calibration liberates the sensor from a tedious calibration process. Therefore, we summarize contributions as follows:

- **Convenient:** Delicate measuring process is designed to routinely calibrate the sensing elastomer's mechanical parameters. It allows for weekly or daily calibration of time-dependent parameters without disassembling the sensor at all.
- **Generalizable:** We propose a practical mechanical parameters calibration method for elastomers of vision-based tactile sensors, which also suits for a wide range of tactile sensors that incorporate built-in deformation measurement capability for their sensing elastomers, thus exhibiting high generalization and broad applicability.
- **Precise:** With the aid of rigorous contact mechanics theory, a standardized experimental process, and a specially customized calibration gauge block, our proposed calibration pipeline can provide accurate estimation of the elastomer's mechanical parameters. This has been validated with both real experiments and simulations.

The rest of this paper is organized as follows: related work on mechanical parameter calibration methods for flexible materials is reviewed in Section II, especially the indentation test. Section III establishes the contact model between the sensing elastomer of the tactile sensor and a flat-ended cylinder indenter, and presents the principle and pipeline of the proposed in-situ calibration. Section IV describes the experimental setup and testing procedure for retrieving precise mechanical parameters of the vision-based tactile sensors, taking GelSlim3.0 [9] as an example. The calibrated parameters are further validated via widely-accepted FEA simulation, and contact force distribution reconstruction using the calibrated parameters is shown in Section V. Finally, we discuss in Section VI and summarize in Section VII.

II. RELATED WORK

In this section, we review different methods that allow calibration of mechanical parameters for elastomers, mainly the indentation test.

A. Standard Calibration Tests

The approaches for determining the elastic modulus and Poisson's ratio of soft material can be mainly divided into dynamic methods and static methods. Dynamic methods obtain mechanical parameters of the sample by measuring its natural vibration frequencies with known shape and density [10]. Static methods, such as the tensile test, compression test, and shear test, measure the stress-strain relationship and the axial strain-transverse strain relationship of the sample in the elastic deformation zone to calculate the elastic modulus and Poisson's ratio.

Nevertheless, the experimental setups and testing procedures of these methods are known to be tedious and time-consuming. For instance, the widely used benchmark for mechanical characteristics calibration, namely the tensile testing, necessitates cutting the tested elastomer into a unique dog-bone-shaped specimen and mounting it onto the corresponding tensile testing machine. Additionally, routine calibration via these techniques is exceedingly challenging when the sensing elastomer is already attached to the vision-based tactile sensor.

B. Indentation Tests

In recent years, indentation tests have been proposed as an alternative to traditional tests for calibrating mechanical properties, due to their convenience [11], [12]. While early theoretical modeling of indentation tests assume that the elastic medium is semi-infinite [13], recent studies have shown that this assumption is not valid in practice. Hayes et al. derive a mathematical solution for Young's modulus of a thin elastic layer with infinite lateral dimensions using a flat-ended cylinder indenter, but their solution only applies to frictionless interfaces and small deformations [14]. Zhang et al. later evaluate the effects of large deformations and friction on indentation tests through simulation, but their method is limited to testing the Young's modulus of soft materials [15]. Jin et al. overcome this limitation by using two different sizes of indenters to simultaneously acquire Young's modulus and Poisson's ratio for the first time [16]. However, the main drawback of these indentation methods is that they require a combination of displacement feedback systems, force transducers, and fixed samples to obtain accurate force-displacement curves, which greatly complicate the preparation process and limit mobility.

Here, we present a novel mechanical parameter calibration method for vision-based tactile sensors that employs flat-end cylindrical indenters and considers appropriate theoretical assumptions. Our approach leverages the deformation measurement capability of the vision-based tactile sensor itself and utilizes a high-precision calibration block, eliminating the need for a bulky displacement feedback system. This leads to a simplified calibration process and significantly improves the accuracy of the results.

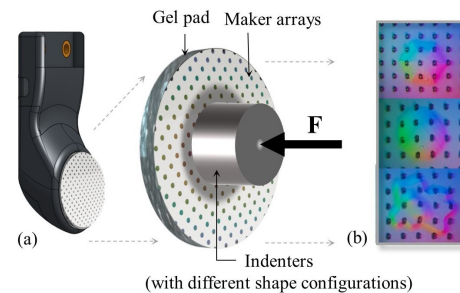


Fig. 2. GelSlim3.0 sensor. (a) Perception mechanism. (b) Tactile images captured by GelSlim3.0.

III. IN-SITU CALIBRATION

To achieve in-situ indentation calibration for vision-based tactile sensors, the contact model between the sensor and indenter is crucial. To this end, we propose some assumptions based on the sensor's structure. The methodology for calculating mechanical parameters using indentation tests is then explained, and the entire pipeline for in-situ calibration of vision-based tactile sensors is demonstrated.

A. Contact Model for Calibration

GelSlim3.0 is a vision-based tactile sensor featuring high resolution, high sensitivity, low cost, durability, convenience and compactness [9]. Its sensing elastomer is a piece of silica gel pad attached to an acrylic prism. Upon contact with objects, the soft gel pad undergoes deformation, while the embedded camera captures tactile images in real-time, as depicted in Fig.2. Although we have chosen GelSlim3.0 as a model for calibration, it is worth noting that our proposed method also works for other tactile sensors equipped with surface sensing elastomers.

Cylindrical indenters are chosen for indentation tests in this work due to their well-defined contact area and more uniform stress distribution, making it easier to derive accurate mechanical properties from the indentation data. Compared to other indenter geometries, such as hemispherical or conical indenters [11], [12], cylindrical indenters offer improved reproducibility and accuracy of results.

By analyzing the structure of GelSlim3.0 and indenters, we can make following assumptions and construct the contact model illustrated in Fig.3.

- The bottom surface of gel pad and the acrylic prism are tightly bonded together, and the stiffness of gel pad is much smaller than that of the acrylic prism, allowing the prism to be simplified as a rigid foundation.
- The boundary conditions of the specimen at lateral boundary can be disregarded during calibration because the radius of the gel pad (15 mm) is 6 times that of indenters (2.5 mm) [17].
- Moreover, unlike the Herzian model's strong assumption of a semi-infinite elastic body, our model takes into account the thickness and deformation of the gel pad.

B. In-situ Calibration Principle

To enable in-situ calibration for vision-based tactile sensors, the indentation test with flat-ended cylindrical indenters—originally employed to access the mechanical properties of biological tissues—is improved in this study. The proposed method is easily accessible and effective with a wide variety of sensing elastomers.

According to Zhang et al. [15], Young's modulus E can be calculated using the formula.

$$E = \frac{1 - \nu^2}{2a\kappa_n(\nu, a/h, w/h)} \cdot \frac{P}{w} \quad (1)$$

where E is the Young's modulus, ν the Poisson's ratio, P the indentation force, w the indentation depth, a the

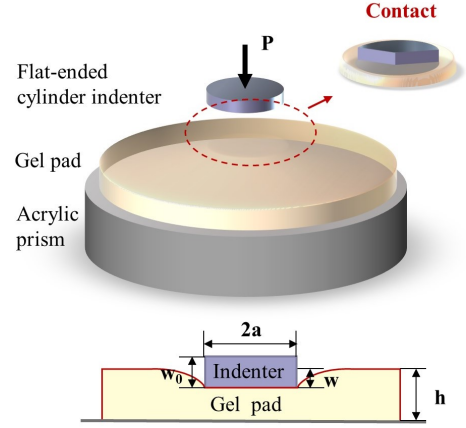


Fig. 3. Simplified contact model of in-situ calibration between the vision-based tactile sensor and the flat-ended cylinder indenter, where P is the indentation force, w the indentation depth, h the thickness of the silicone gel pad, a the radius of the cylindrical indenter.

indenter's radius, h the tested material's thickness, κ_n a factor that depends on aspect ratio a/h , Poisson's ratio ν , and deformation ratio w/h . From $\kappa_n(\nu, a/h)$, the dependence of $\kappa_n(\nu, a/h, w/h)$ on w/h is approximately linear:

$$\kappa_n(\nu, a/h, w/h) = \kappa(\nu, a/h) \cdot (1 + \beta \frac{w}{h}) \quad (2)$$

where β is a factor depends on the aspect ratio and Poisson's ratio (i.e., $\beta = \beta(\nu, a/h)$) and describes the dependency of $\kappa_n(\nu, a/h, w/h)$ on w/h . The β table can be built by corresponding the $\kappa_n(\nu, a/h, w/h)$ values from [15] with different a/h and ν .

Substituting (2) into (1) yields:

$$\frac{P}{w} = \frac{2aE\kappa(\nu, a/h)}{1 - \nu^2} \cdot (1 + \beta \frac{w}{h}) \quad (3)$$

Define

$$c = \frac{2aE\kappa(\nu, a/h)}{1 - \nu^2} \quad (4)$$

So (3) can be rewritten as:

$$\frac{P}{w} = c\beta \cdot \frac{w}{h} + c \quad (5)$$

where the slope $c\beta$ and the y-intercept c can be obtained by data fitting, allowing for the determination of Poisson's ratio by looking up the β table. The Young's modulus can then be calculated using (4). The specific calculation process will be shown in section IV later.

C. In-situ Calibration Pipeline

Fig. 4 presents an overview of the comprehensive pipeline for conducting in-situ calibration. The experimental setup comprises a vision-based tactile sensor, force/torque sensor, robot arm, and flat-ended cylindrical indenters. The force/torque sensor facilitates the acquisition of precise force data while the vision-based tactile sensor ensures consistent

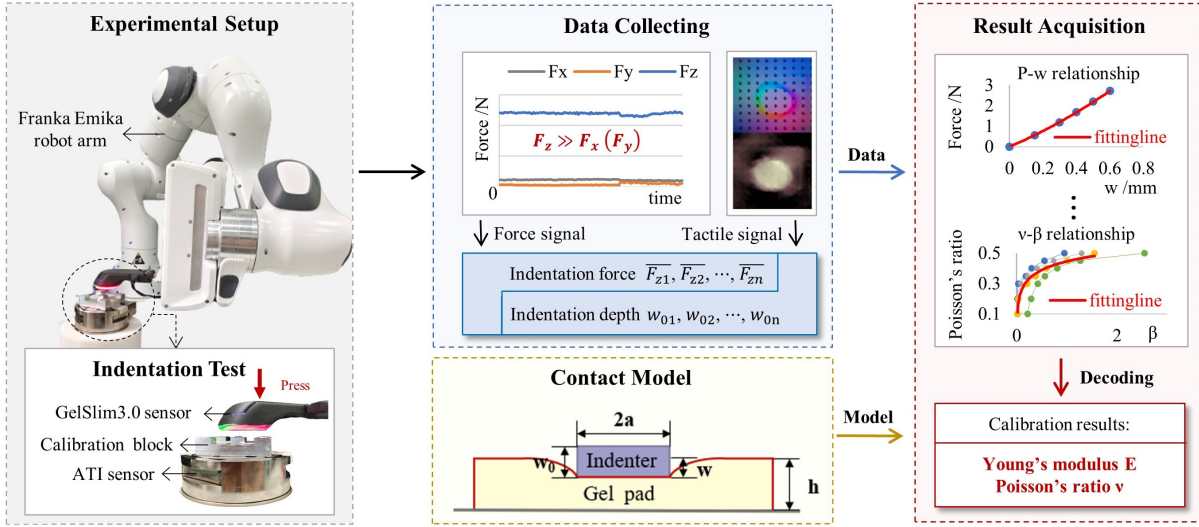


Fig. 4. In-situ calibration pipeline. Standardized experimental procedures, rigorous contact mechanics theory, and sufficient data ensure that this pipeline can provide accurate estimation of mechanical parameters for vision-based tactile sensors.

indentation depths in line with the predetermined CNC-ed thickness of the indenters. Finally, the acquired data is fitted to a force-deformation curve, enabling the accurate decoupling of Young's modulus and Poisson's ratio based on the relevant contact model and indentation principles.

IV. EXPERIMENT VALIDATION

We validate the proposed framework of in-situ calibration with specific experiments. Here, a customized calibration gauge block ensures the accuracy of experimental results.

1) *Experiment Setup*: The platform shown in Fig.4 (left) is set up to calibrate mechanical parameters of the vision-based tactile sensor.

A high-precision force/torque sensor (ATI-IA) with a measurement precision of 1/160 N in the x/y direction and 1/80 N in the z direction is employed in this study. To ensure accurate and reliable measurements, a CNC-machined gauge block with five flat-ended cylindrical indenters, specially customized with a machining error of less than 10 μm , is utilized. All indenters have a 2.5 mm radius and a depth range of 0 to 0.6 mm, which is within 20% of the tested elastomer thickness. The bevel incision adjacent to each indenter is utilized to ensure that the indentation depth is accurately reached, and the absolute height of the gauge block is measured with a contact profiler, as shown in Fig.5. To facilitate repeated pressings during calibration, the Franka Emika robot arm is employed. Nevertheless, this robot's displacement accuracy only marginally meets the calibration requirements. As a result, a precise motion stage is actually used to impose indentation with a higher degree of accuracy, and we advise using more precise displacement-controlled robotic arms for subsequent indentation tests.

2) *Calibration procedure*: First, fix the GelSlim3.0 sensor on the robot's end effector with screws, and tightly adhere the block with the testing indenter to the ATI force/torque sensor

to avoid the indenter's rigid displacement. After determining the distance between the indenter and the GelSlim3.0 sensor, control the robot's motion to guarantee consistent displacement at each test. Simultaneously, watch the tactile images of the sensor and the resultant force values detected by the ATI sensor. When the beveled incision next to the cylindrical indenter just shows up in the tactile image, and the tangential resulting force values F_x , F_y are greatly lower than the pressure value F_z , record the normal force that corresponds to the pre-defined accurate indentation depth (i.e., $w = w_0$), as shown in Fig.4 (center).

To reduce random errors in sampling, we drive the robot to repeat the operation ten times for the same indentation depth, sample 200 sets of force data for each operation, and take the average result finally. When pressing repeatedly, the indenter should preferably be in contact with different positions on the surface of the gel pad, so as to eliminate the influence of local uneven composition of the elastomer.

3) *Data processing*: Paired indentation force P and indentation depth w can be obtained by experiments, and the parameters used in data processing also include: the thickness of the gel pad $h = 3.0$ mm, the radius of cylindrical

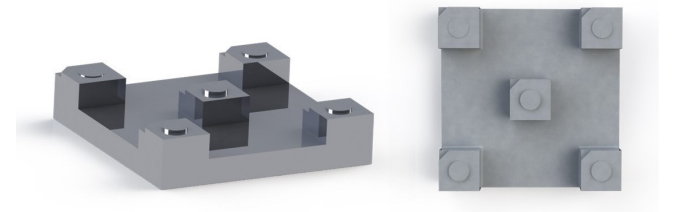


Fig. 5. A precise CNC machining calibration gauge block, including 5 flat-ended cylinder indenters and adjacent bevel incisions, which thickness are 0.15, 0.3, 0.4, 0.5, 0.6 mm.

indenter $a = 2.5$ mm, the standard indentation depth $w_0 \in \{0.15, 0.3, 0.4, 0.5, 0.6\}$ mm. According to the relationship curve between indentation force P and deformation w in Fig.6 (a), a linear relationship between P/w and w/h can be fitted as follows:

$$\frac{P}{w} = 5.2662 \cdot \frac{w}{h} + 3.4943 \quad (R^2 = 0.9999) \quad (6)$$

Since c is the y-intercept, $c\beta$ is the slope, $c = 3.4943$ and $\beta = 1.5071$ can be obtained from (5). In this work, the β table is plotted as a series of relational curves with data from Zhang et al.'s research [15], as shown in Fig.6 (b). Substitute the aspect ratio ($a/h = 0.8$) in this experiment, the relationship curve between the factor β and Poisson's ratio ν under this aspect ratio is:

$$\nu = 0.0813 \ln \beta + 0.4464 \quad (R^2 = 0.9842) \quad (7)$$

Substituting $\beta = 1.5071$ into (7) yields $\nu = 0.4797$. From (4), the elastic modulus can also be calculated using the measured c, ν, a, h data and the $\kappa(\nu, a/h)$ data published by Hayes [14], where c can be regarded as the indentation hardness P/w when $w/h \rightarrow 0$, we get $E = 0.1981$ MPa.

Therefore, mechanical parameters of the GelSlim3.0 sensor are obtained through in-situ calibration, where the Poisson's ratio $\nu = 0.4797$, and the Young's modulus $E = 0.1981$ MPa.

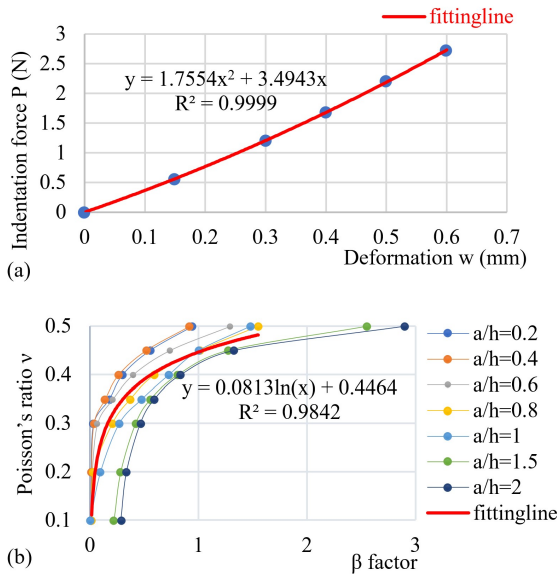


Fig. 6. (a) Indentation force P and deformation w relationship curve. (b) Poisson's ratio ν and factor β relationship curve series, with data from [15].

V. FURTHER VALIDATION

A. Simulation Validation

The Abaqus/Standard FEA simulation is used in this section to validate the accuracy of mechanical parameters obtained from in-situ calibration. The reason we rely on simulation here that it's challenging to actually acquire the

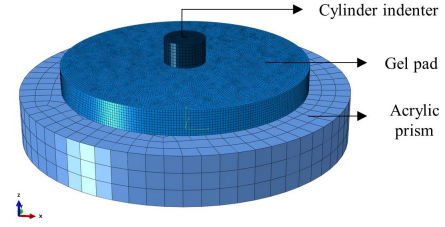


Fig. 7. Initial FEA simulation configuration (meshed).

calibration results with the traditional experiments since the GelSlim3.0 sensor has been fully assembled, peeling off the attached gel pad will damage the sensor, and the same batch of silica gel as the current gel pad is not accessible now. On the other hand, the real experiment is time-consuming, which we'll leave to the next phase [18].

The core idea is to compare the deformations of the sensing elastomer in the simulation, using the calibrated E and ν for the material properties, to that of actual tests while applying the same amount of force onto the indenter. In this study, we use the Neo-Hookean hyperelastic model, which is widely used to model elastomers. Furthermore, the usage of linear elastic or hyperelastic constitutive models has little impact on the finite element analysis of elastomers within the small deformation range of vision-based tactile sensors. This means that the theory of linear elasticity can also be effectively applied to the principle of in-situ calibration.

As illustrated in Fig.7, the silicone gel pad is modeled as a thin cylinder, 30 mm in diameter and 3 mm in height. To improve computational efficiency without compromising accuracy, a simplified 2D model is subsequently utilized in the simulation, given that all objects are central-symmetric.

a) Material properties: Based on the experimental measurement results, the mechanical parameters of silica gel are determined as $E = 0.1981$ MPa, $\nu = 0.4797$, and the Neo-Hookean hyperelastic model provided by Abaqus is assigned to silica gel here. The model parameters are converted to $C_{10} = 0.0335$, $D_1 = 1.2297$. Additionally, the linear elastic model parameters for the cylindrical indenter and acrylic plate are set as $E = 210$ Gpa, $\nu = 0.3$ and $E = 3$ Gpa, $\nu = 0.32$, respectively.

b) Interaction and loading: The contact between gel pad and cylindrical indenter is modeled as a hard contact with a friction coefficient of 0.3, and discretized with a surface-to-surface method. The gel pad and acrylic are directly tied together. The designed amount of force is loaded downward from top surface of cylindrical indenter.

c) Mesh: The element type used here is the simplified integration hexahedral 8-node element (C3D8R), and the mesh of sensing elastomer is refined.

Here, Fig.8 (a) and (c) reveal that the Abaqus simulation results for normal deformation match well with the experimental indentation depths at both qualitative and quantitative levels, with a relative error of less than 6%. In addition, the force-deformation curves obtained from 20 frames of force

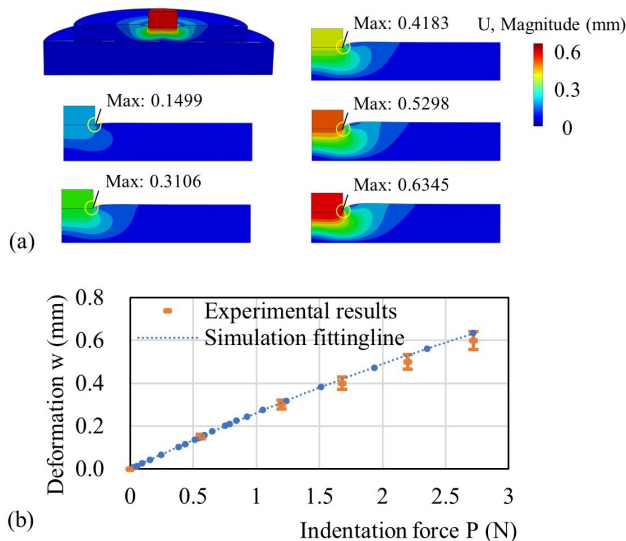


Fig. 8. Simulation results. (a) 3D and 2D displacement deformation contours. (b) Experimental results (orange dots) and FEA simulation results (blue dots and curve) of the relationship. (c) Quantitative comparison between actual indentation depths and simulation deformations.

and displacement data in simulation are compared with the actual experimental results in Fig.8 (b), and good agreement is observed. These results indicate that the in-situ calibration method for the mechanical parameters of the vision-based sensor is accurate.

B. Force Reconstruction Validation

Reliable mechanical properties of soft sensing elastomers are essential for numerous fundamental research and practical applications. To highlight the contribution of the mechanical parameters acquired through calibration, we modify and utilize the inverse finite element method described in [4] to precisely estimate the three-dimensional contact force distribution, as shown in Fig.9.

VI. DISCUSSIONS

We discuss several precautions for carrying out the in-situ calibration.

1) *Deformation control*: It is recommended to limit the deformation of the sensing elastomer to within twenty percent during the calibration process. If the elastomer's deformation is too large, the initially apparent linear relationship between the mechanical parameters and the deformation may not hold (e.g., $\kappa_n(v, a/h, w/h) = \kappa(v, a/h) \cdot (1 + \beta w/h)$, and the sensor may be damaged as well.

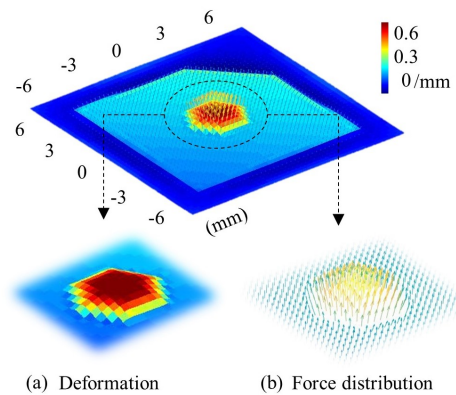


Fig. 9. 3D contact force distribution reconstructed by calibrated mechanical parameters. (a) Deformation and (b) force distribution in the central area.

2) *Repeating and waiting*: For this calibration procedure, it is recommended to average several measurements and to wait between each measurement. Sufficient waiting time between two indentation experiments is necessary to allow the elastomer surface to fully recover to its initial state. Otherwise, the measured stiffness of the second trial may be slightly larger.

3) *Sensors with non-flat surface*: The proposed in-situ calibration is also applicable for tactile sensors with non-planar surfaces (e.g., the TacTip family [19]). The only additional step is to measure and calculate the equivalent thickness of the elastomer.

VII. CONCLUSIONS

Since Young's modulus and Poisson's ratio, which may change with time, are the two vital mechanical parameters that describe a soft material's deformation under external or internal loads, and routinely estimating the two parameters is essential for force reconstruction in tactile sensors. In this paper, we propose an in-situ calibration, with which people can retrieve the mechanical parameters of the elastomer for vision-based tactile sensors, both accurately and conveniently. This approach lays the groundwork for the tactile sensors' force-related perception.

Any calibration method for mechanical parameters would require three components: deformation measurement, force measurement, and models to retrieve E and ν from the measurements. Core to the proposed in-situ mechanical calibration method is that: (1) Deformation is accurately measured using the sensor's sensing capability with the help of precise CNC machined indentation blocks; (2) Force is accurately measured using an external force/torque sensor; (3) E and ν can be untangled by a two-step "fitting-calculating" procedure built with solid contact mechanics foundation.

The simulation results and contact force distribution reconstruction demonstrate the accuracy and potential of the proposed in-situ calibration method.

REFERENCES

- [1] W. Yuan, S. Dong, and E. H. Adelson, "GelSight: High-resolution robot tactile sensors for estimating geometry and force," *Sensors*, p. 2762, 2017.
- [2] H. Sun, K. J. Kuchenbecker, and G. Martius, "A soft thumb-sized vision-based sensor with accurate all-round force perception," *Nature Machine Intelligence*, pp. 135–145, 2022.
- [3] M. Lambeta, P.-W. Chou, S. Tian, B. Yang, B. Maloon, V. R. Most, D. Stroud, R. Santos, A. Byagowi, G. Kammerer, D. Jayaraman, and R. Calandra, "DIGIT: A novel design for a low-cost compact high-resolution tactile sensor with application to in-hand manipulation," *IEEE Robotics and Automation Letters*, pp. 3838–3845, 2020.
- [4] D. Ma, E. Donlon, S. Dong, and A. Rodriguez, "Dense Tactile Force Estimation using GelSlim and inverse FEM," in *2019 International Conference on Robotics and Automation (ICRA)*, pp. 5418–5424, 2019.
- [5] Q. Li, O. Kroemer, Z. Su, F. F. Veiga, M. Kaboli, and H. J. Ritter, "A review of tactile information: perception and action through touch," *IEEE Transactions on Robotics*, pp. 1619–1634, 2020.
- [6] S. Ito, N. Hirai, and Y. Ohki, "Changes in mechanical and dielectric properties of silicone rubber induced by severe aging," *Ieee Transactions on Dielectrics and Electrical Insulation*, vol. 27, no. 3, pp. 722–730, 2020.
- [7] V. Placet and P. Delobelle, "Mechanical properties of bulk polydimethylsiloxane for microfluidics over a large range of frequencies and aging times," *Journal of Micromechanics and Microengineering*, vol. 25, p. 035009, 03 2015.
- [8] R. Hopf, L. Bernardi, J. Menze, M. Zündel, E. Mazza, and A. E. Ehret, "Experimental and theoretical analyses of the age-dependent large-strain behavior of Sylgard 184 (10:1) silicone elastomer," *Journal of the Mechanical Behavior of Biomedical Materials*, pp. 425–437, 2016.
- [9] I. Taylor, S. Dong, and A. Rodriguez, "GelSlim3.0: High-resolution measurement of shape, force and slip in a compact tactile-sensing finger," 2021.
- [10] M. J. Treacy, T. W. Ebbesen, and J. M. Gibson, "Exceptionally high young's modulus observed for individual carbon nanotubes," *nature*, pp. 678–680, 1996.
- [11] M. Tani, A. Sakuma, and M. Shinomiya, "Evaluation of thickness and Young's modulus of soft materials by using Spherical Indentation Testing," *Transactions of the Japan Society of Mechanical Engineers. A*, pp. 901–908, 2009.
- [12] M. Dao, N. Chollacoop, K. J. Van Vliet, T. A. Venkatesh, and S. Suresh, "Computational modeling of the forward and reverse problems in instrumented sharp indentation," *Acta Materialia*, pp. 3899–3918, 2001.
- [13] H. Hertz, *Miscellaneous papers*. London: Macmillan, New York, Macmillan and co., 1896.
- [14] W. C. Hayes, L. M. Keer, G. Herrmann, and L. F. Mockros, "A mathematical analysis for indentation tests of articular cartilage," *Journal of Biomechanics*, pp. 541–551, 1972.
- [15] M. Zhang, Y. P. Zheng, and A. F. T. Mak, "Estimating the effective Young's modulus of soft tissues from indentation tests—nonlinear finite element analysis of effects of friction and large deformation," *Medical Engineering & Physics*, pp. 512–517, 1997.
- [16] H. Jin and J. L. Lewis, "Determination of Poisson's ratio of articular cartilage by indentation using different-sized indenters," *Journal of Biomechanical Engineering*, pp. 138–145, 2004.
- [17] R. L. Spilker, J.-K. Suh, and V. C. Mow, "A finite element analysis of the indentation stress-relaxation response of linear biphasic articular cartilage," *Journal of biomechanical engineering*, pp. 191–201, 1992.
- [18] C. T. McKee, J. A. Last, P. Russell, and C. J. Murphy, "Indentation versus tensile measurements of young's modulus for soft biological tissues," *Tissue Engineering Part B: Reviews*, vol. 17, no. 3, pp. 155–164, 2011. PMID: 21303220.
- [19] B. Ward-Cherrier, N. Pestell, L. Cramphorn, B. Winstone, M. E. Giannaccini, J. Rossiter, and N. F. Lepora, "The TacTip family: soft optical tactile sensors with 3D-printed biomimetic morphologies," *Soft robotics*, pp. 216–227, 2018.